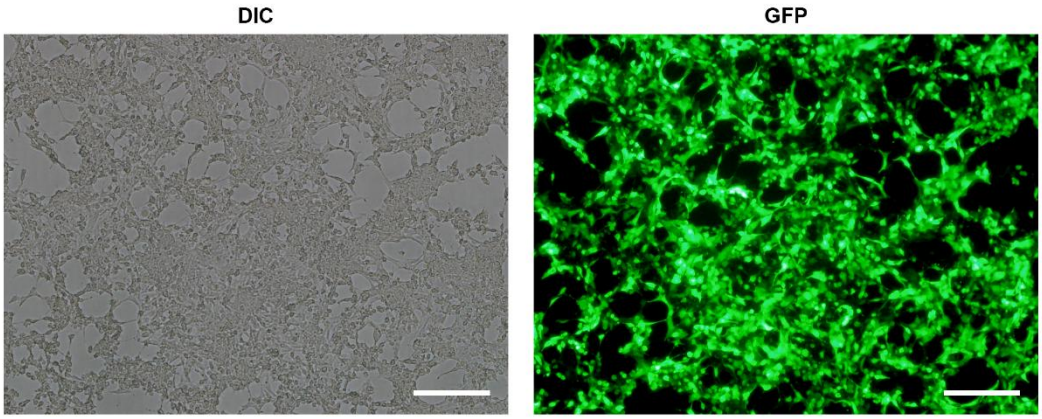

Figure S1. Packaging of lentivirus encoding anti-CD205 scFv protein, related to Figure 2. After the plasmid encoding anti-CD205 scFv protein was co-transfected with the helper plasmids into 293T cells for 24 hours, the lentiviral packaging efficiency was reflected by fluorescence expression in 293T cells observed by inverted fluorescence microscopy. Experiments were independently performed in triplicate, yielding consistent results. Scale bar: 100 μm.

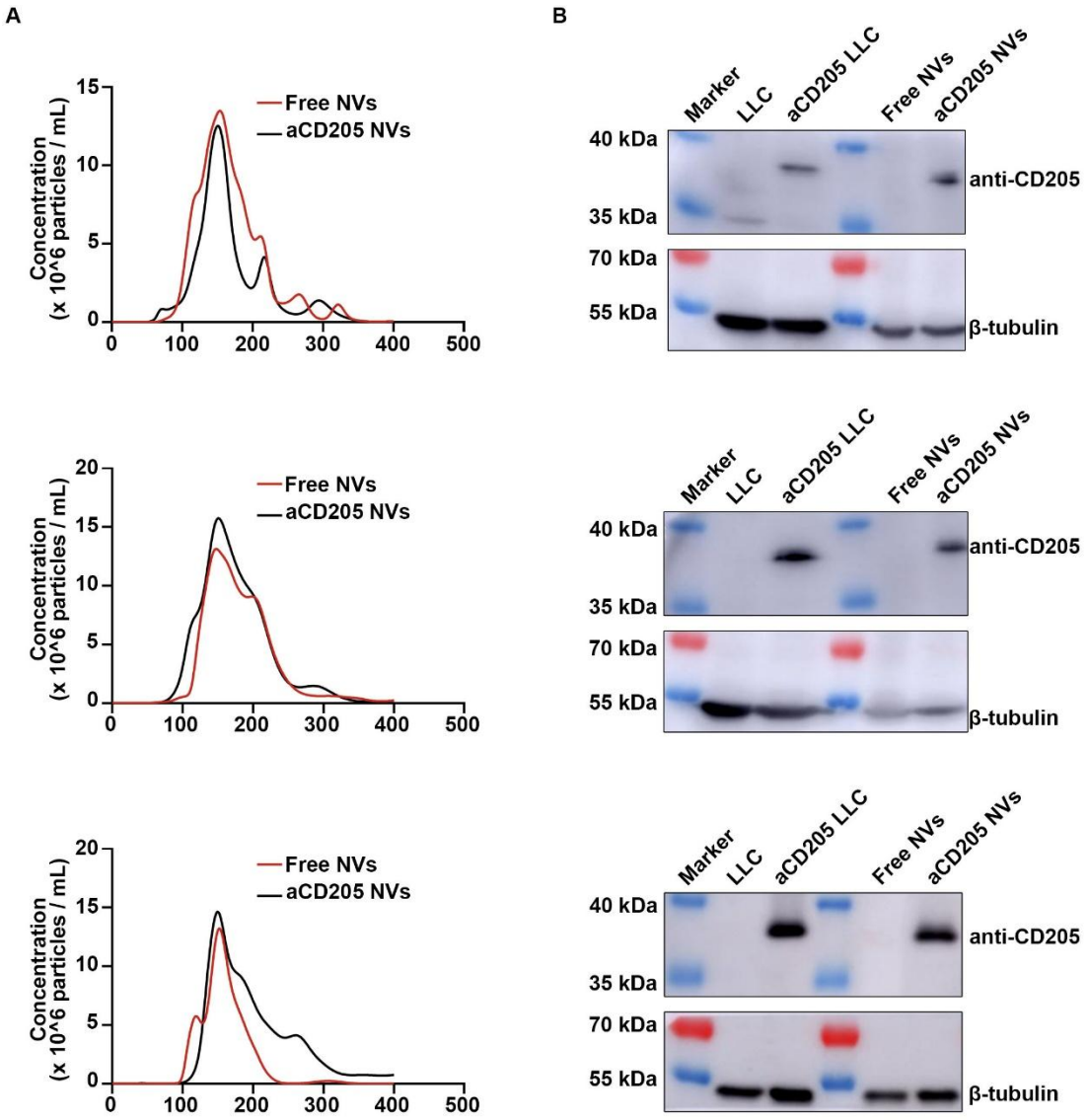

Figure S2. Batch-to-batch consistency of aCD205 NVs, related to Figure 2. (A) Particle size of aCD205 NVs from three independent batches were analyzed by NTA. **(B)** Western blot analysis of anti-CD205 scFv in aCD205 LLC cells and corresponding NVs from three independent batches.

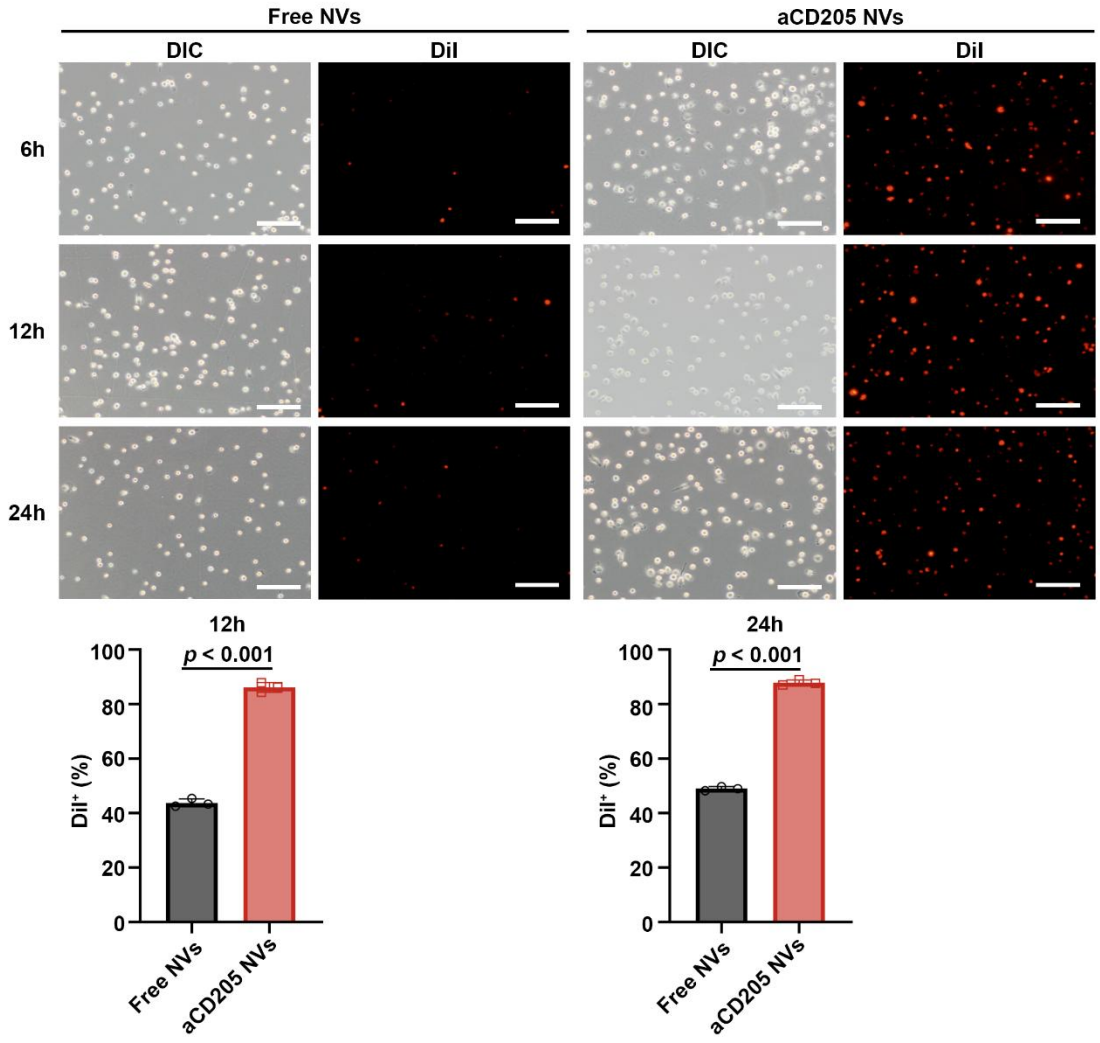

Figure S3. aCD205 NVs uptake by BMDCs, related to Figure 3. Representative images and statistical analysis showing DiI-labeled NVs uptake by BMDCs after co-culturing for 6, 12, and 24 hours. Scale bar: 100 μm. Experiments were independently performed in triplicate, yielding consistent results. Data are expressed as mean (SD). Statistical significance was calculated by an unpaired two-tailed Student's *t* test.

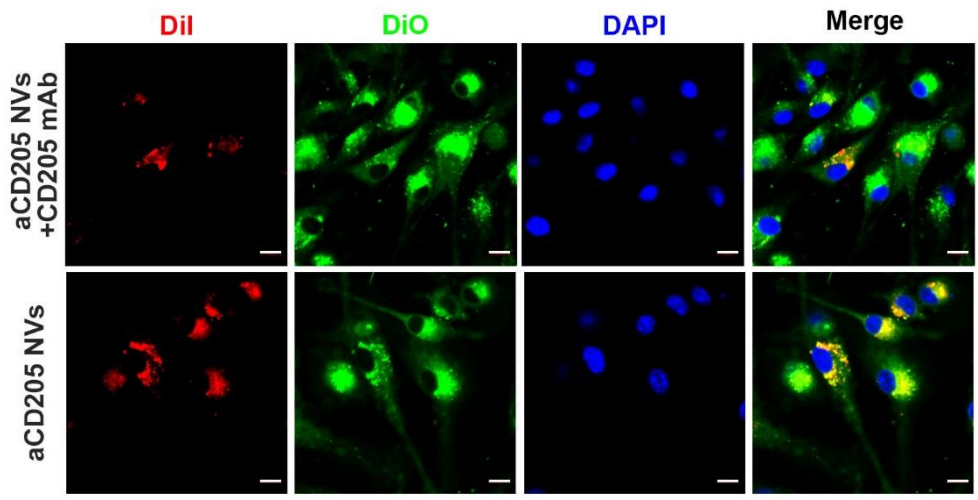

Figure S4. Blocking experiment where the BMDCs are stained with or without preincubation of the aCD205 mAb, related to Figure 3. Confocal microscopy showing a specific, CD205-mediated uptake of aCD205 NVs by BMDCs after coincubation. DiI for aCD205 NVs (red), DiO for BMDCs (green), DAPI for nuclei (blue). Scale bar: 10 μm.

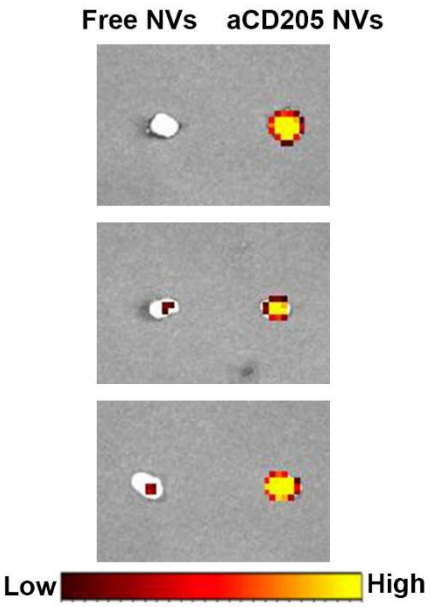

Figure S5. IVIS images of lymph nodes from mice treated with different NVs (n=3), related to Figure 3. 24 hours after footpad injection of DiR-labeled aCD205 NVs and Free NVs, inguinal LNs were resected and visualized by IVIS.

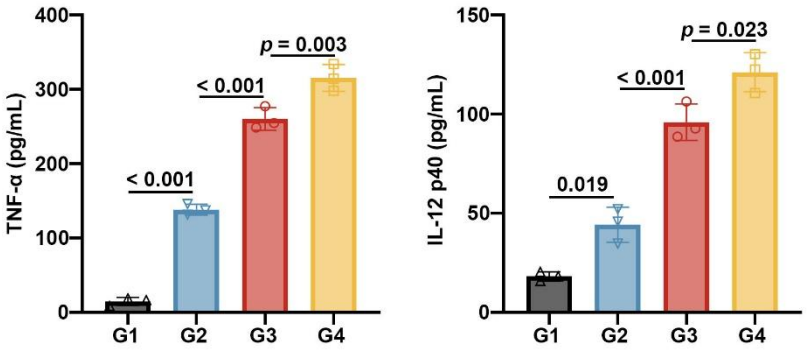

Figure S6. Statistical analysis of cytokine secretion profile of BMDCs following co-culture, related to Figure 3. Levels of TNF-α and IL-12p40 in the supernatant of BMDCs after co-culture with PBS (G1), Free NVs (G2), aCD205 NVs (G3) and LPS (G4) were quantified by ELISA. Data are presented as mean (SD). Statistical significance was calculated by one-way ANOVA with Tukey's post hoc test.

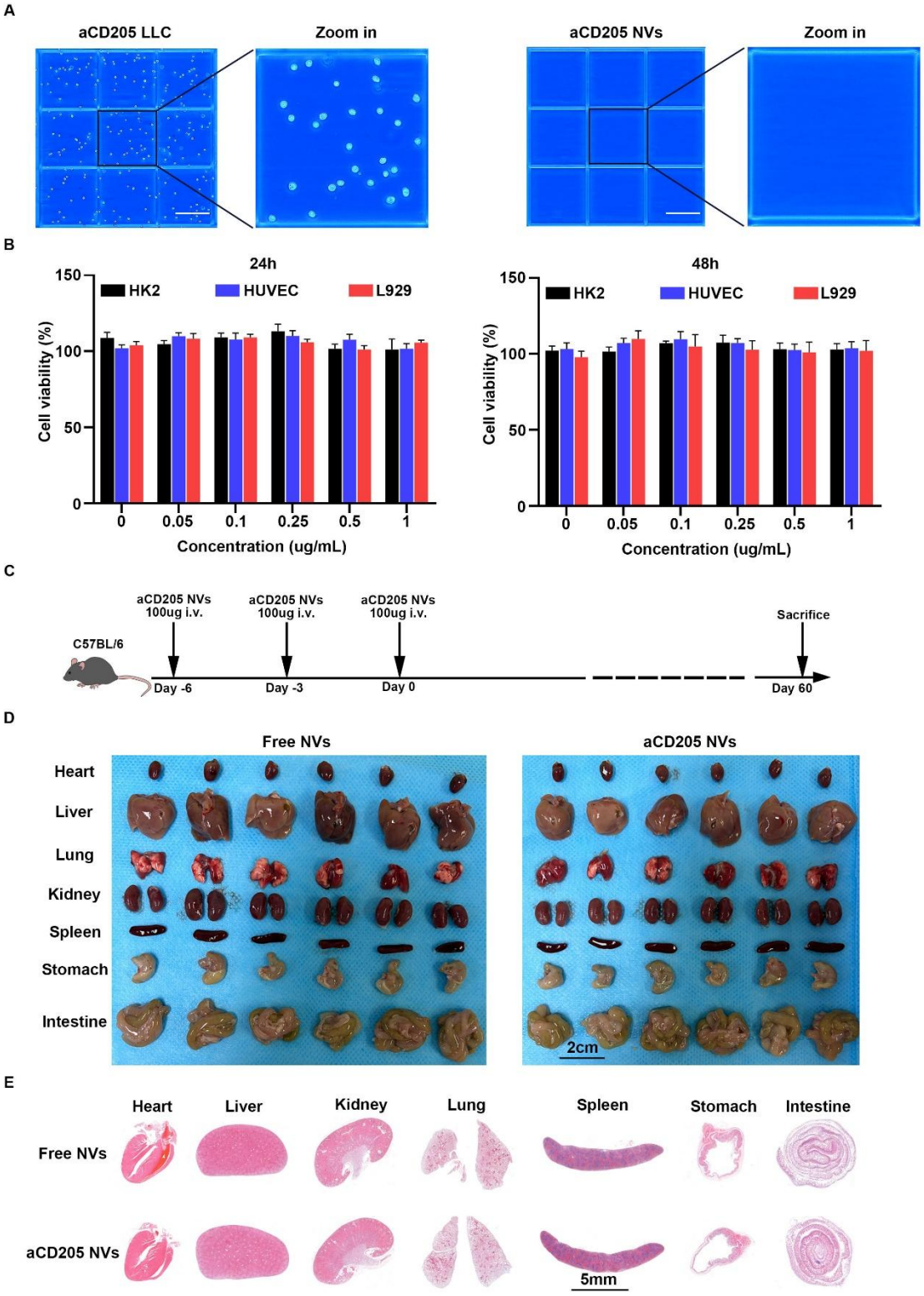

Figure S7. Safety evaluation of aCD205 NVs *in vitro* and *in vivo* (n=6). (A) Representative image of microscopic examination confirming the absence of viable cells in the aCD205 NVs preparation. Scale bar: 200 μm. **(B)** Assessment of the effect of aCD205 NVs on the viability of HK2, HUVEC, and L929 cells using the CCK-8 assay. **(C)** Schematic of the *in vivo* administration regimen: Healthy C57BL/6 mice received intravenous injections of aCD205 NVs (100 μg per dose) every three days for

three times. Major organs (heart, liver, lung, kidney, spleen, stomach and intestine) were harvested 60 days after the final administration. **(D)** Gross photographs (scale bar: 2 cm) and **(E)** representative H&E-stained sections (scale bar: 5 mm) of major organs from the mice.

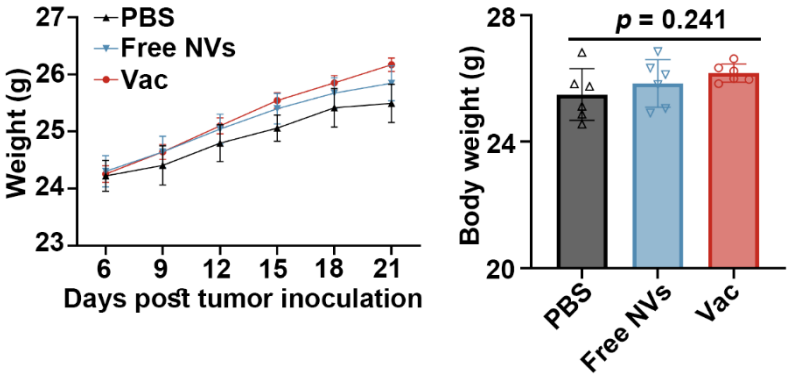

Figure S8. Body weight change and statistical analysis of mice after *i.v.* injection of PBS, Free NVs, and Vac (n=6), related to Figure 4. Data are presented as mean (SD). Statistical significance was calculated by one-way ANOVA with Tukey's post hoc test.

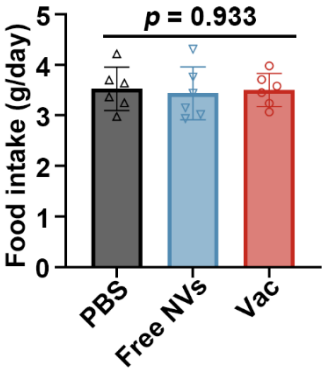

Figure S9. Food intake of mice after *i.v.* injection of PBS, Free NVs, and Vac (n=6), related to Figure 4. Data are presented as mean (SD). Statistical significance was calculated by one-way ANOVA with Tukey's post hoc test.

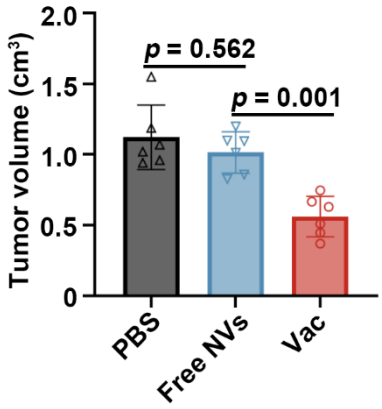

Figure S10. Statistical analysis of the final tumor volume of mice after *i.v.* injection of PBS, Free NVs, and Vac (n=6), related to Figure 4. Data are presented as mean (SD). Statistical significance was calculated by one-way ANOVA with Tukey's post hoc test.

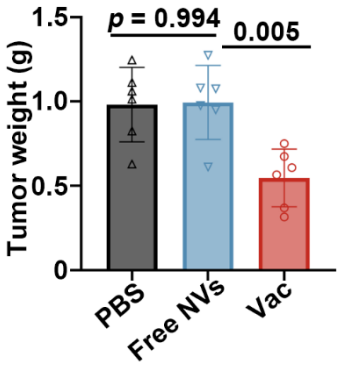

Figure S11. Statistical analysis of the tumor weight of mice after *i.v.* injection of PBS, Free NVs, and Vac (n=6), related to Figure 4. Data are presented as mean (SD). Statistical significance was calculated by one-way ANOVA with Tukey's post hoc test.

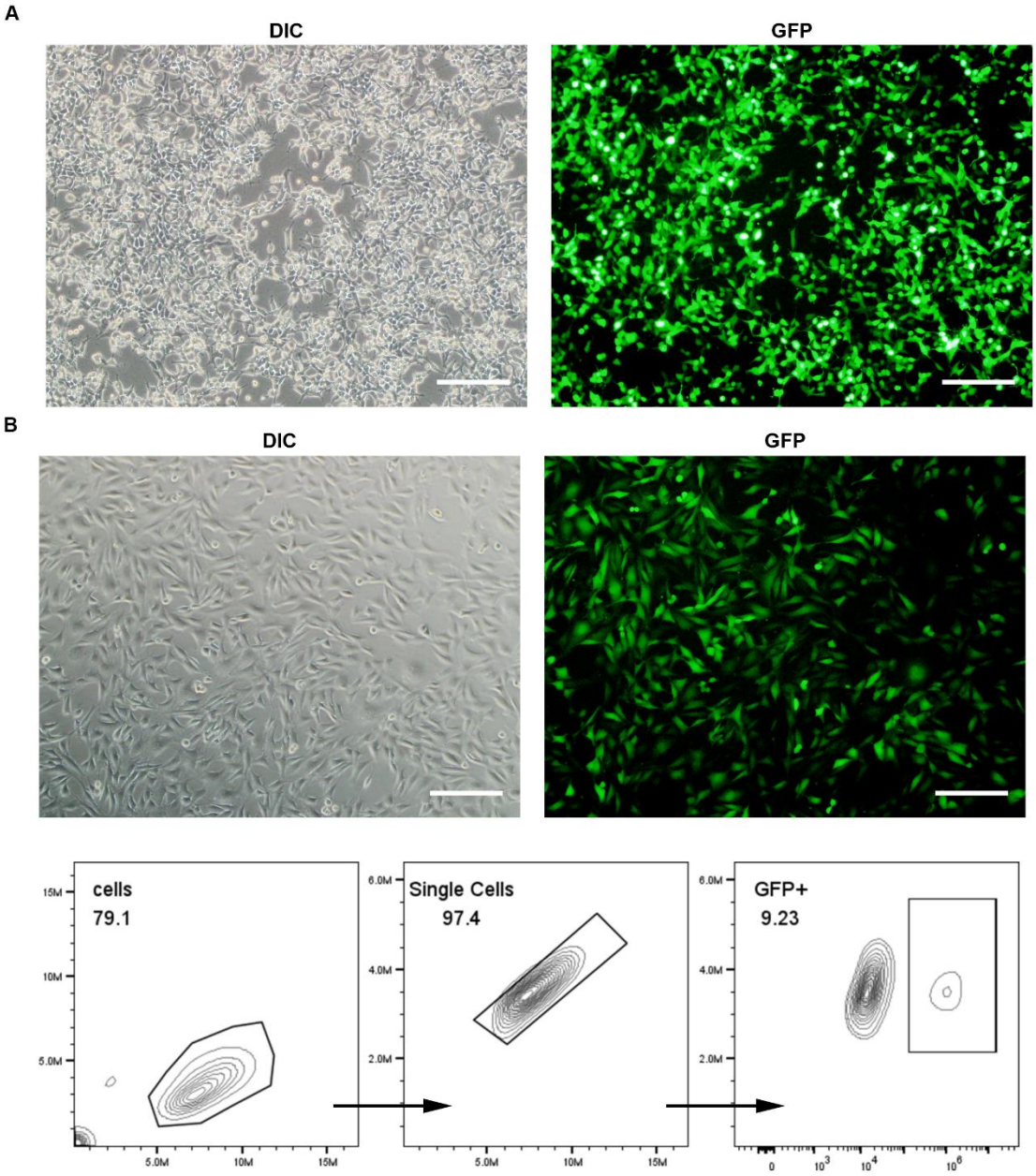

Figure S12. Packaging and titration of retrovirus encoding CAR protein, related to Figure 5. (A) After the MSCV-CAR plasmid was co-transfected with the pCL-eco plasmid into Plat-E packaging cells for 24 hours, retroviral packaging efficiency was reflected by fluorescence expression in Plat-E cells observed by inverted fluorescence microscopy. **(B)** Forty-eight hours subsequent to the retrovirus infection of NIH-3T3 cells, the retrovirus titer was determined through flow cytometry. The percentage of GFP-positive cells was analyzed for wells exhibiting 1%–10% GFP-positive cells. Experiments were independently performed in triplicate, yielding consistent results. Scale bar: 100 μm.

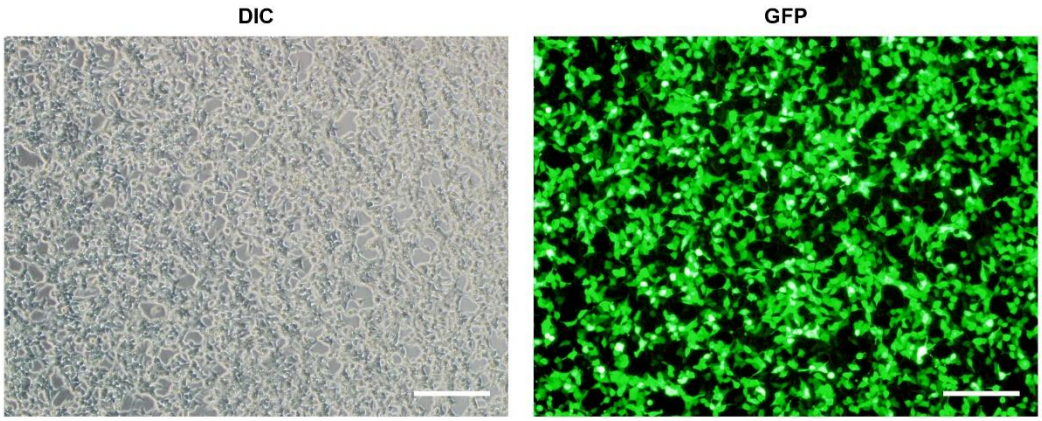

Figure S13. Packaging of lentivirus encoding MSLN protein, related to Figure 5. After co-transfection of MSLN protein encoding plasmid and helper plasmids into 293T cells for 24 hours, lentiviral packaging efficiency was reflected by fluorescence expression in 293T cells observed by inverted fluorescence microscopy. Experiments were independently performed in triplicate, yielding consistent results. Scale bar: 100 μm.

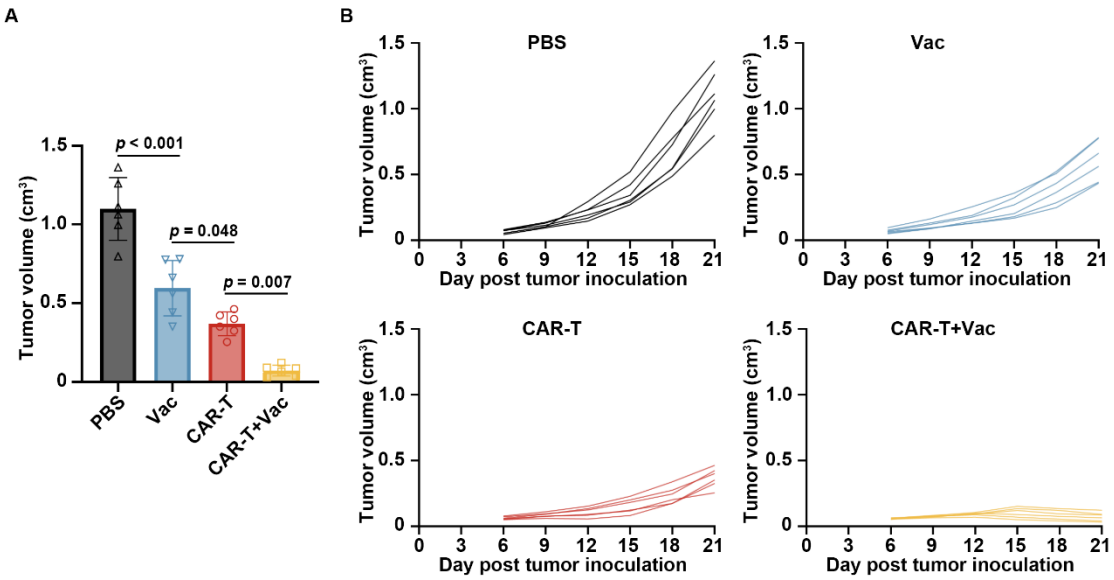

Figure S14. Tumor volume and tumor growth curves of individual subcutaneous tumor-bearing mice after *i.v.* injection of PBS, Vac, CAR-T, and CAR-T Vac (n=6), related to Figure 6. (A) Tumor volume statistical analysis of four groups. **(B)** Individual tumor growth curves across treatment groups (n = 6). Data are presented as mean (SD). Statistical significance was calculated by one-way ANOVA with Tukey's post hoc test.

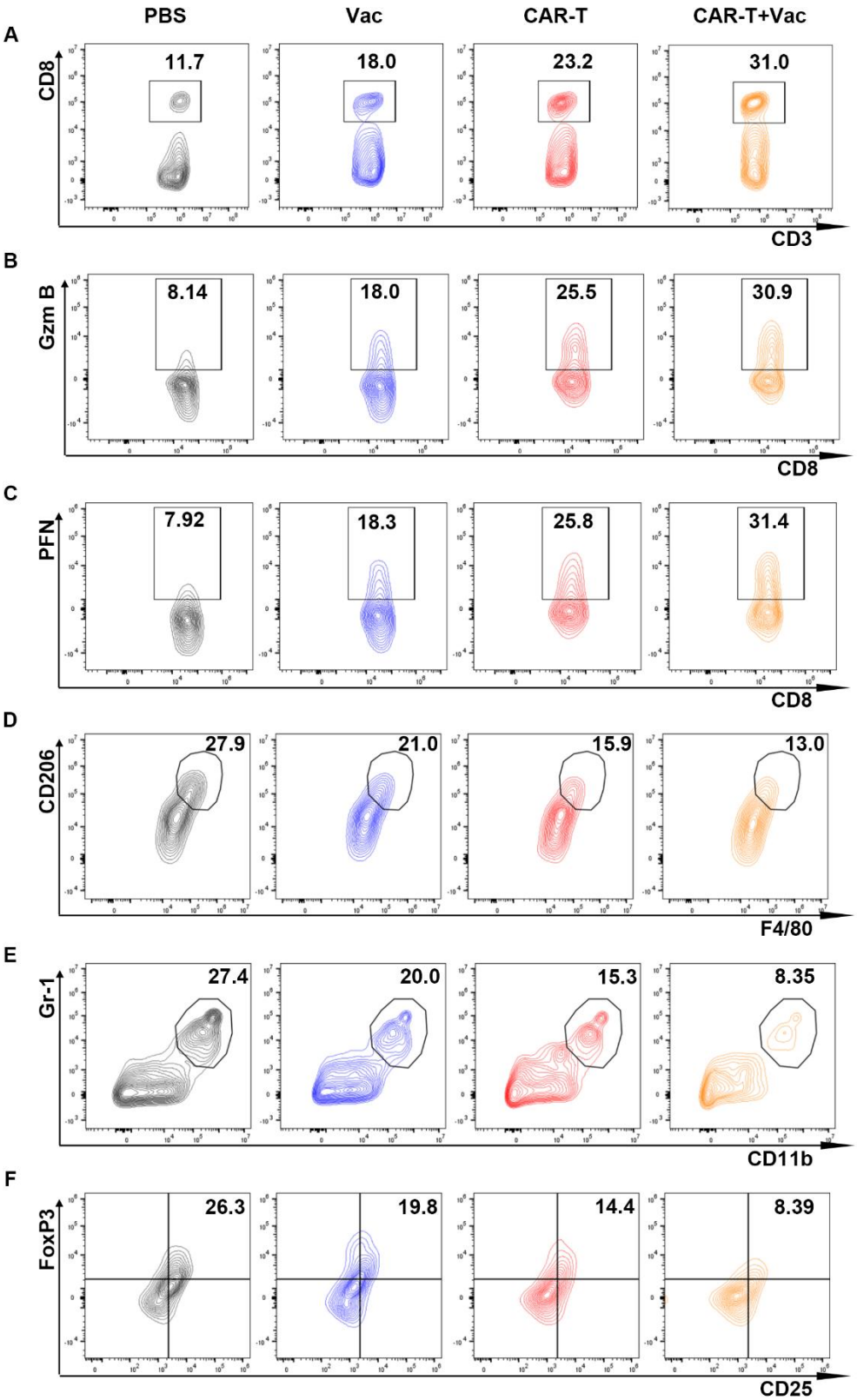

Figure S15. TME analysis of subcutaneous tumor-bearing mice after *i.v.* injection of PBS, Vac, CAR-T, and CAR-T Vac (n=6), related to Figure 6. Representative flow cytometry plots: **(A)** tumor-infiltrating $CD8^+$T cells, **(B)** granzyme B and **(C)** perforin generation $CD8^+$T cells, **(D)** M2 macrophages, **(E)** MDSCs, and **(F)** Tregs within the TME.

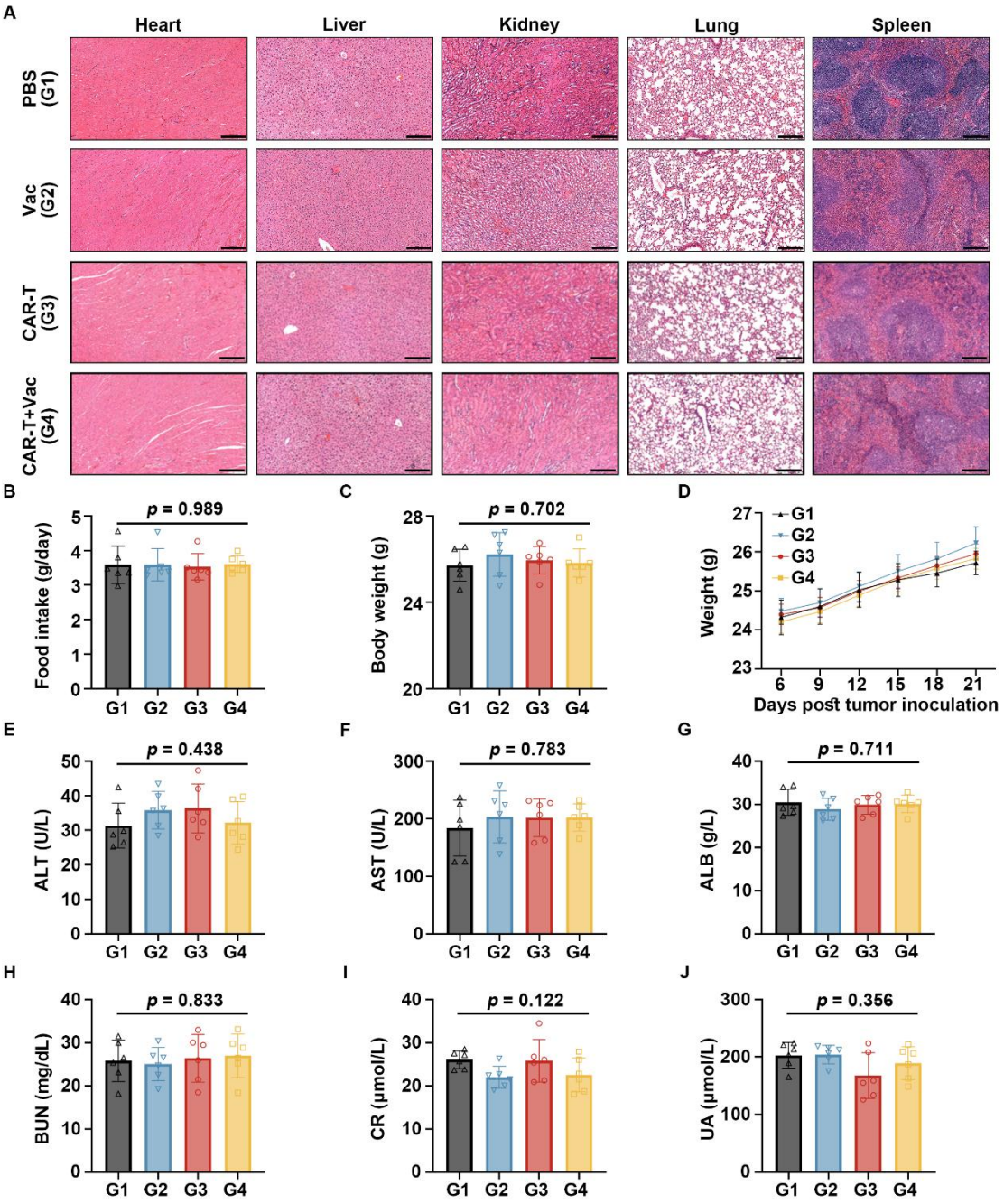

Figure S16. Biosafety evaluation of the CAR-T+Vac therapy (n=6), related to Figure 6. (A) Representative H&E staining of the organs from mice after various treatments. Scale bar: 200 μm. **(B)** Food intake per mouse per day across different treatment groups. **(C)** Body weight of mice prior to sacrifice. **(D)** Body weight changes of mice over the treatment period. **(E)-(J)** Blood biochemical indexes analysis (ALT, AST, ALB, UREA, CREA, UA) after different treatments. Data are presented as mean (SD). Statistical significance was calculated by one-way ANOVA with Tukey's post hoc test.

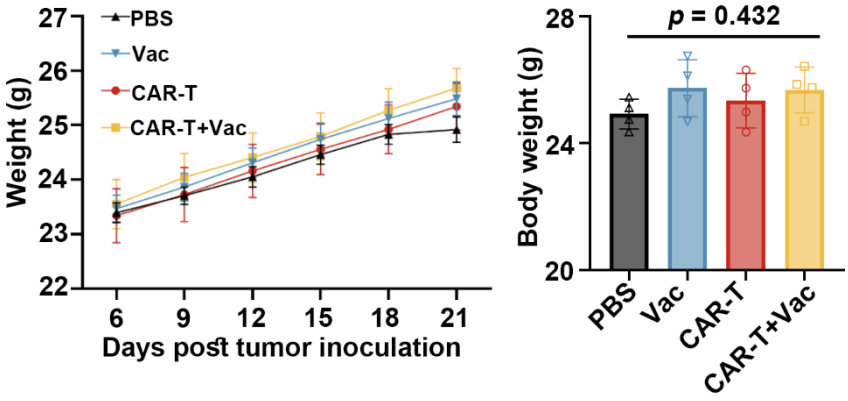

Figure S17. Body weight change and statistical analysis of orthotopic tumor-bearing mice after *i.v.* injection of PBS, Vac, CAR-T, and CAR-T+Vac (n=6), related to Figure 7. Data are presented as mean (SD). Statistical significance was calculated by one-way ANOVA with Tukey's post hoc test.

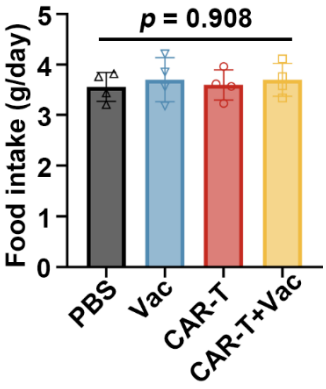

Figure S18. Food intake of orthotopic tumor-bearing mice after *i.v.* injection of PBS, Vac, CAR-T, and CAR-T+Vac (n=6), related to Figure 7. Data are presented as mean (SD). Statistical significance was calculated by one-way ANOVA with Tukey's post hoc test.

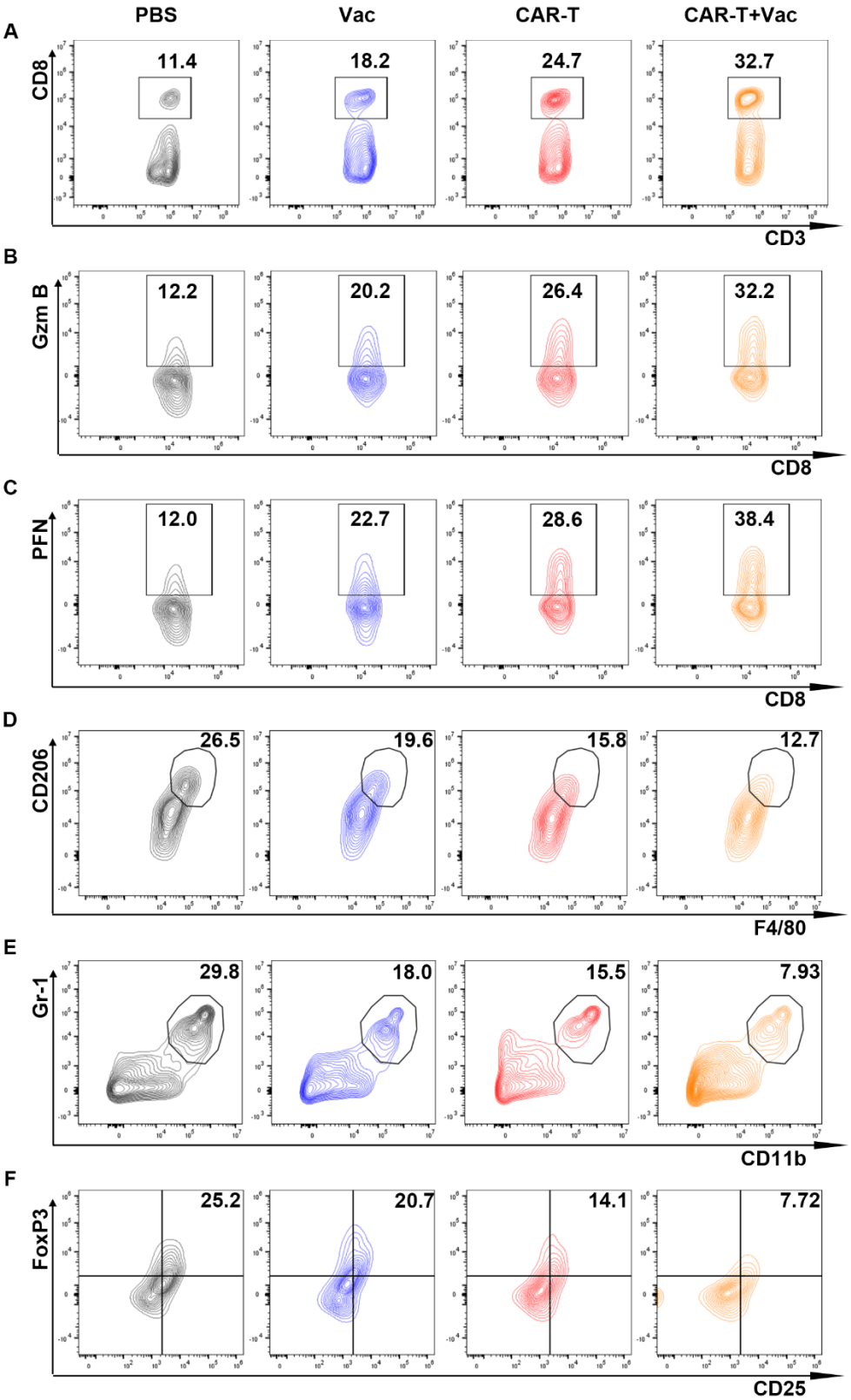

Figure S19. TME analysis of orthotopic tumor-bearing mice after *i.v.* injection of PBS, Vac, CAR-T, and CAR-T+Vac (n=4), related to Figure 7. Representative flow cytometry plots: **(A)** tumor-infiltrating $CD8^+$T cells, **(B)** granzyme B and **(C)** perforin generation $CD8^+$T cells, **(D)** M2 macrophages, **(E)** MDSCs, and **(F)** Tregs within the TME across different treatment groups.